



Long Non-coding RNA ASNR Targeting miR-519e-5p Promotes Gastric Cancer Development by Regulating FGFR2

Zihao Chen^{1,2}, Yong Li^{2*}, Bibo Tan², Fang Li³, Qun Zhao², Liqiao Fan², Zhidong Zhang², Xuefeng Zhao², Yu Liu² and Dong Wang²

¹ Graduate School of Hebei Medical University, Shijiazhuang, China, ² The Third Department of Surgery, The Fourth Hospital of Hebei Medical University, Shijiazhuang, China, ³ Department of Pathology, The Fourth Hospital of Hebei Medical University, Shijiazhuang, China

OPEN ACCESS

Edited by:

Yongbin Chen,
Kunming Institute of Zoology (CAS),
China

Reviewed by:

Chaohong Liu,
Huazhong University of Science
and Technology, China
Shuang Liu,
Central South University, China

Shengtao Zhou,
Sichuan University, China

*Correspondence:

Yong Li
li_yong_hbth@126.com

Specialty section:

This article was submitted to
Molecular and Cellular Oncology,
a section of the journal
Frontiers in Cell and Developmental
Biology

Received: 11 March 2021

Accepted: 10 June 2021

Published: 09 July 2021

Citation:

Chen Z, Li Y, Tan B, Li F, Zhao Q,
Fan L, Zhang Z, Zhao X, Liu Y and
Wang D (2021) Long Non-coding
RNA ASNR Targeting miR-519e-5p
Promotes Gastric Cancer
Development by Regulating FGFR2.
Front. Cell Dev. Biol. 9:679176.
doi: 10.3389/fcell.2021.679176

Gastric cancer (GC), as a common gastrointestinal tumor, is an important cause of death from cancer all around the world. Long non-coding RNAs (lncRNAs), a novel class of transcripts, have attracted great attention of researchers. However, the mechanisms of the clinical significance of most lncRNAs in human cancer are mainly undocumented. This research desires to explore the clinical significance, biological function, and mechanism of Lnc_ASNR (apoptosis suppressing-non-coding RNA) in GC. Cell proliferation, cell cycle, cell migration, and invasion abilities were respectively determined by 3-(4,5)-dimethylthiazolium (-z-y1)-3,5-di-phenyltetrazolium bromide (MTT), flow cytometry, wound healing, and Transwell assay (Sigma-Aldrich, St. Louis, MO, United States). The association of Lnc_ASNR, miR-519e-5p, and fibroblast growth factor receptor 2 (FGFR2) was evaluated *via* luciferase reporter experiments. The tumor xenograft assay was conducted to confirm the results of cell experiments. High expressed Lnc_ASNR was detected in both GC cells and tissues using qRT-PCR. Downregulated Lnc_ASNR could reduce proliferation, migration, and invasion in GC cells, while upregulated Lnc_ASNR could promote the cell proliferation, migration, and invasion. Moreover, the effect of Lnc_ASNR on migration and invasion ability is closely related to epithelial-mesenchymal transition (EMT). The bioinformatics analysis, luciferase assay, and Western blot demonstrated that Lnc_ASNR inhibited miR-519e-5p expression but increased FGFR2 expression. Lnc_ASNR and FGFR2 were both targeted to miR-519e-5p, and they were negatively correlated with the expression of miR-519e-5p. All investigations indicated that Lnc_ASNR functioned as a ceRNA targeting miR-519e-5p and facilitated GC development by regulating the pathway of miR-519e-5p/FGFR2.

Keywords: gastric cancer, long non-coding RNA, Lnc_ASNR, proliferation, invasion, migration

Abbreviations: GC, gastric cancer; lncRNAs, long non-coding RNAs; qRT-PCR, quantitative real-time PCR; MTT, 3-(4,5)-dimethylthiazolium (-z-y1)-3,5-di-phenyltetrazolium bromide; EMT, epithelial-mesenchymal transition; FGFR, fibroblast growth factor receptor; nt, nucleotides; ceRNA, competitive endogenous RNA; TNM, tumor-node-metastasis; si-NC, negative control siRNA; GFP, green fluorescent protein; RIPA, radio immunoprecipitation assay; OS, overall survival; CIC, cancer-initiating cells.

INTRODUCTION

Gastric cancer (GC) is a prevalent malignant tumor around the world with the sixth incidence rate and second mortality rate, which seriously affects human health (Bray et al., 2018). The advanced diagnosis and therapy of GC has achieved development in recent years. However, many limitations existed that hinder the effectiveness of GC treatment. The early symptoms of most GC patients are not obvious, and diagnosis delay becomes the main obstacle of GC treatment and prognosis. The combination of gastroscopy and biopsy is the universally recognized gold standard for GC diagnosis (Virgilio et al., 2017; den Hollander et al., 2019). However, its application in GC screening is still limited because it is not easy to be accepted by patients due to the invasiveness and high cost. At present, the most commonly used tumor biomarkers in clinical are insufficient to completely replace biopsy, so it is of great significance to explore more specific and sensitive biomarkers for early diagnosis of GC to improve the clinical treatment effect.

Long non-coding RNA (lncRNA) is an RNA molecule with a length between 200 and 100,000 nucleotides (nt), which can be transcribed independently. lncRNA is molecularly similar to mRNA, but there is no identifiable potential to encode functional proteins (Ulitsky, 2016). Researchers confirmed that lncRNA contains a significant biological function among several diseases (Montes et al., 2021; Zhang F. et al., 2021; Zhang Y. et al., 2021; Zhu et al., 2021). It is related to tumor development, chemotherapy sensitivity, and prognosis and especially plays a vital role in the resistance of multiple tumor chemotherapy drugs, especially in GC (Zhang and Wang, 2021), prostate cancer (Shang et al., 2019), and pancreatic cancer (Zhou et al., 2020). The expression of lncRNA is abnormal in a wide range of cancers. lncRNA demonstrates an essential influence in facilitating and inhibiting cancer occurrence and development, which proves its clinical potential as a biomarker and therapeutic target (Kim et al., 2018; Ramnarine et al., 2019; Wang Y. L. et al., 2019; Olivero et al., 2020). Recent findings indicated that lncRNA can interact with proteins, RNA, and lipids, thereby producing cancer signal transduction (Lin and Yang, 2018). In addition, lncRNAs, as competing endogenous RNAs (ceRNAs) or microRNA sponge, can regulate expression by competitively binding to microRNA (Song et al., 2017; Sun et al., 2017; Huang et al., 2019). Researchers have found that most lncRNAs are upregulated or downregulated expressly in tissues and serum plasma of patients with GC (Zhang et al., 2018; Wang C. J. et al., 2019; Guo et al., 2020; Yuan et al., 2020). Therefore, lncRNA can be used as a potential tumor marker for GC diagnosis.

Lnc_ASNR (non-coding RNA that inhibits apoptosis) is a nuclear-reserved lncRNA. Lnc_ASNR located in the chr14-q22.2 region is a newly discovered lncRNA associated with cancer and other diseases. Compared with normal tissues, Lnc_ASNR expression is significantly increased in four tumor tissues. Chen's group (Chen et al., 2016) has found that Lnc_ASNR promotes the reduction of cytoplasmic AUF1 levels and inhibits AUF1-mediated degradation of Bcl-2 mRNA in colon cancer RKO cells, which leads to high expression of Bcl-2 and significantly inhibits cell apoptosis. However, the role and mechanism of Lnc_ASNR

in tumorigenesis and development are unclear, which suggested that the study of the impact of Lnc_ASNR on tumors remains to be explored. Herein, we first evaluated whether Lnc_ASNR changes in the expression of lncRNA in GC and further clarified the biological function of Lnc_ASNR and the molecular mechanism that regulates the occurrence and development of GC. The research results help to identify important molecules that effectively regulate the occurrence and development of GC, which will provide a theoretical basis for clinical molecular diagnosis of GC and the development of targeted drugs. Our results exhibit important scientific significance and potential clinical application value for improving patient prognosis and enhancing survival rate.

MATERIALS AND METHODS

Clinical and Histologic Evaluation of Human Tissues

In this study, 76 paired tumor tissues and adjacent non-tumor tissues were collected from GC patients at the Fourth Hospital of Hebei Medical University from 2017 to 2020. The GC diagnosis was histopathologically confirmed. Clinical pathological features, including gender, age, tumor-node-metastasis (TNM) staging, and tumor size, were summarized. None of them received preoperative treatment, including chemotherapy or radiotherapy. After obtaining the tissues, the samples were immediately placed in liquid nitrogen and then stored at -80°C . The research was approved by the Research Ethics Committee at the Fourth Hospital of Hebei Medical University (Shijiazhuang, China). All patients were informed and gave their consent.

Cell Culture

Four GC cell lines (MKN45, MKN28, AGS, and HGC27) and gastric mucosal epithelial cell (GES-1) were purchased from the Cell Bank of the Chinese Academy of Sciences (Shanghai, China). All cells were cultured in Roswell Park Memorial Institute (RPMI) 1640 medium (GIBCO, Thermo Fisher Scientific, Waltham, MA, United States) containing 10% fetal bovine serum (FBS) (BI, 100 U/ml penicillin, and 100 mg/ml streptomycin (Invitrogen, Thermo Fisher Scientific) at 37°C with 5% CO_2 .

RNA Extraction and Quantitative Real-Time PCR

RNAiso Plus (TaKaRa, Tokyo, Japan) was utilized to extract total RNA from cells and tissue samples according to manufacturer's information. The OD260/OD280 ratio ranging from 1.9 to 2.1 tested by UV spectrophotometer is qualified. Reverse transcription polymerase chain reaction was performed by LnRctue lncRNA First-Strand cDNA kit (TIANGEN, Beijing, China) and LnRctue lncRNA qPCR kit (SYBR Green) (TIANGEN) for quantitative real-time PCR (qRT-PCR) according to manufacturer's information. ABI 7500 real-time PCR system (Applied Biosystems, Waltham, MA, United States) was utilized to conduct qRT-PCR and collect data. GAPDH was used as a loading control. Our qRT-PCR results were analyzed

and expressed relative to threshold cycle (C_t) values, and then converted to fold changes. The specific primer sequences used in our study are provided in the **Supplementary Table 1**.

Vector Construction and Transfection and siRNA Transfection

Based on manufacturer's information, Lipofectamine 2000 (Invitrogen) was used to transfect plasmid vectors and siRNAs into GC cells. The plasmid vector pcDNA3.1 used for Lnc_ASNR overexpression in MKN28, the siRNA (three individual ASNR siRNAs) used for Lnc_ASNR knockdown in MKN45 cells, miR-519e-5p inhibitor, and miR-519e-5p mimics, and the negative control (vector or NC) were obtained from Invitrogen. To upregulate ASNR, the coding sequence was increased based on the manufacturer's instructions and subcloned into the pcDNA3.1 (+) vector (Invitrogen). Then Lipofectamine 2000 (Invitrogen) was used to transfect MKN28 cells with a negative control vector or a ASNR-expressed plasmid. In order to downregulate ASNR, Lipofectamine 2000 (Invitrogen) was utilized to transfect MKN28 cells with the target sequence of negative control siRNA. After being transfected for 48 h, cells were obtained for qRT-PCR and Western blot experiments. The siRNA sequences used in our study are provided in the **Supplementary Table 2**.

Lentiviral Infection

The MKN45 cell suspension was seeded onto a six-well plate at concentration of 3×10^4 cells/well, and the cells were grown to a density of 20%. We have created two different groups, sh-ASNR transfected with shASNR green fluorescent protein (GFP) lentivirus and shNC (GENECHEM) transfected with empty GFP lentivirus, respectively. An appropriate amount of lentivirus was added according to the differences in infection (MOI = 20). After 3 days of transfection, a fluorescence microscope was used to observe GFP-tagged gene expression. Cells with transfection efficiency > 80% were selected for further analyses.

Cell Proliferation Assays

The cell viability of MKN45 cells transfected with si-ASNR and MKN28 cells transfected with pcDNA3.1-ASNR was evaluated *via* MTT Cell Proliferation and Cytotoxicity Assay Kit (Solarbio, Beijing, China) based on the manufacturer's guidance. Transfected MKN-45 cells and MKN28 cells (5×10^4 /well) were incubated with MTT (20 μ l/well) at 37°C for 4 h. Next, DMSO was added and mixed for 10 min to ensure the crystals were dissolved. The optical density value was measured at the absorbance 570 nm under Thermo Scientific Microplate Reader Multiskan MK3 (Thermo Fisher Scientific).

Flow Cytometry for Cell Cycle Analysis

si-ASNR- or si-NC-transfected MKN45 cells and pcDNA3.1-ASNR- or blank vector-transfected MKN28 cells were obtained after 48 h of transfection by Lipofectamine 2000 (Invitrogen). Next, the cells were dyed with propidium iodide (PI) utilizing the DNA content quantitative measurement method (cell cycle

(Solarbio) and detected *via* FACScan. Calculate and compare the percentage of cells in G0/G1, S, and G2/M phases.

Wound-Healing Assay

To conduct the wound healing experiment, 3×10^5 cells were seeded into six-well plates and cultured overnight. Cells were transfected with pcDNA3.1-ASNR, si-ASNR, and si-NC, respectively. When the cultured cells reached a density of 90%, a sterile 10-ml disposable pipette tip was used to produce uniform scratches. The cells were then grown in a medium containing 1% FBS for 48 h. At indicated time points, a microscope was used to obtain images of the plate (Olympus, Tokyo, Japan). Meanwhile, scratch area and wound-healing percentage were calculated. The experiment was repeated three times in parallel.

Cell Migration and Invasion Assays

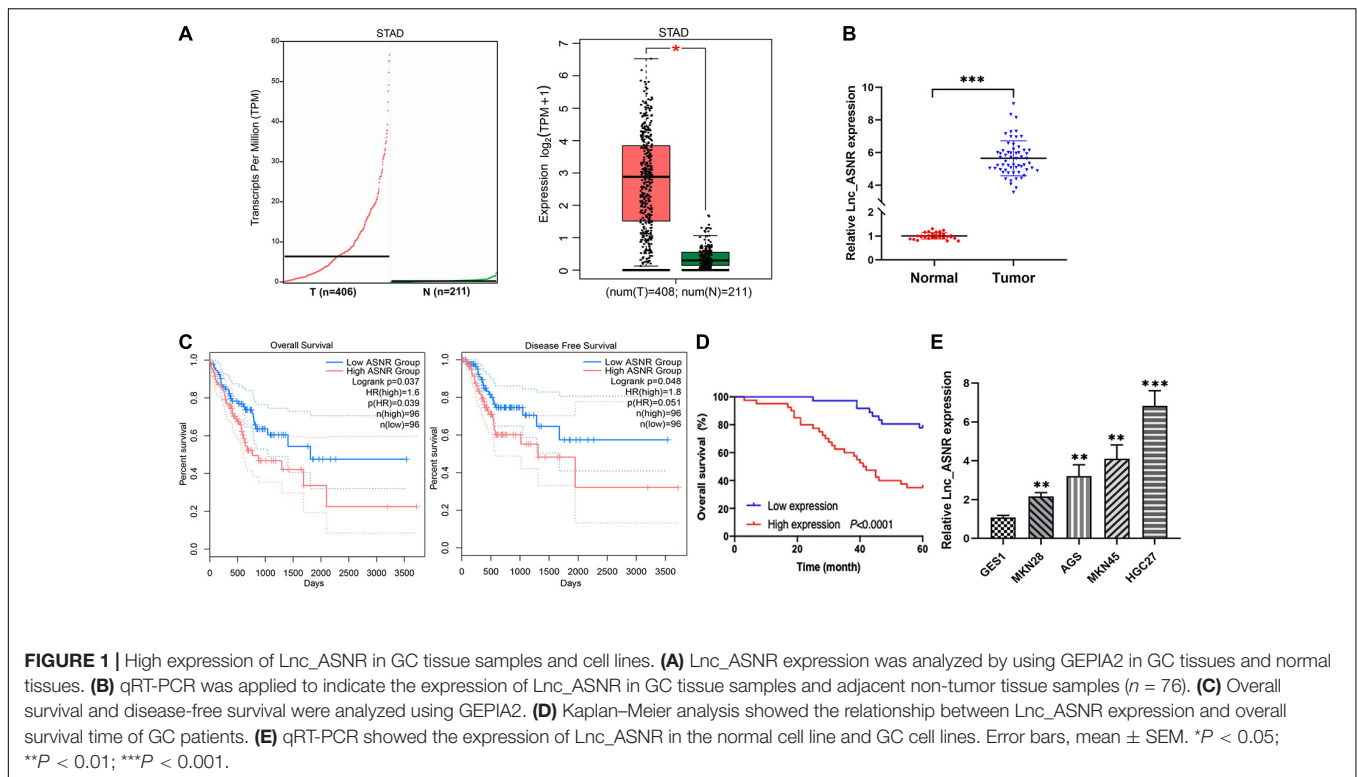
si-ASNR- or si-NC transfected MKN45 cells and pcDNA3.1-ASNR-transfected MKN28 cells were harvested after 48 h of transfection and then collected. Twenty-four-well Transwell plates (8 μ m pore size) (Corning Inc, Corning, NY, United States) were applied for cell migration and invasion assays. Briefly, 50 μ l of Matrigel was placed into the Transwell upper chambers (Sigma-Aldrich). Cells (1×10^5) suspended in 100 μ l of serum-free culture medium were seeded into the upper chambers. Added RPMI 1640 culture medium supplemented with 10% FBS into the wells under the chamber. The cells were cultured in the medium for 48 h at 37°C with 5% CO₂. Then, a cotton swab was utilized to wipe away the remaining cells on the membrane. Cells migrated or invaded through the membrane were stained with methanol and 0.1% crystal violet. Cells were then imaged and counted using an IX71 inverted microscope (Olympus). Five random fields were counted in each well. The experiment was repeated three times in parallel.

Western Blot Assay and Antibodies

Radio immunoprecipitation assay (RIPA) protein lysis buffer (Solarbio) supplemented with protease inhibitor cocktail (Roche, Basel, Switzerland) and phenylmethylsulfonyl fluoride (Roche) was applied for protein extraction. The proteins concentration was evaluated through a BCA Protein Assay Kit (Solarbio). Ten percent sodium dodecyl sulfate-polyacrylamide gel electrophoresis (SDS-PAGE) was used to detach protein extracts (50 μ g). The protein extracts were transferred to 0.22 mm polyvinylidene fluoride membranes (Sigma), then incubated with specific antibodies. ECL chromogenic substrate was applied to evaluate the specific bands. The specific bands were then quantified by densitometry (Quantity One software, Bio-Rad) with β -actin used as a control. All antibodies (1:2,000 dilutions) were purchased from Abcam (Cambridge, United Kingdom).

Luciferase Reporter Assay

The 3'-UTR of human FGFR2 or Lnc_ASNR was amplified from human genomic DNA and individually inserted into a pGL3-basic vector (Promega, Madison, WI, United States). The fragment of FGFR2 or lncRNA-ASNR 3'-UTR mutant was then inserted into the pGL3-basic vector (Promega) control vector



at the same position. To perform the reporter experiments, transfect MKN45 cells with wild-type or mutant reporter plasmid and miR-519e-5p mimic by Lipofectamine 2000 (Invitrogen). After 36 h of transfection, the luciferase activities and the firefly luciferase vitalities were detected under Dual-Luciferase® Reporter Assay System (Promega). They were normalized based on Renilla luciferase activity.

Immunohistochemistry

Formalin and paraffin were used to fix and embed the isolated tumor tissues, respectively. The tissue examples were then cut into 5 mm thick. Immunochemical staining was performed following the standard protocol. Tumors from mice were immunostained for H&E, Ki67. Inverted microscope (Nikon, Tokyo, Japan) was applied to capture the staining intensities of Ki67, and ImageJ software was used to analyze the data. Anti-Ki67 (1:50) was purchased from Roche.

Xenograft Study

All experiments were approved by the Committee on the Ethics of Animal Experiments of Hebei Medical University. The investigations were conducted strictly on the basis of the recommendations in the *Guide for the Care and Use of Laboratory Animals of the National Institutes of Health*. MKN45 cells were stably infected with control shRNA or sh-ASNR using lentiviruses. GC cells were injected into either side of the armpit regions of the male BALB/c nude mice. The mice (4–5 weeks old) were randomly divided into two groups ($n = 6/\text{group}$). Tumor volumes and weights were measured every 3 days, and tumor volumes were measured regularly. Calculate as the

equation: $V = 0.5 \times D \times d^2$ (V , volume; D , longest diameter; d , diameter perpendicular to the longest diameter). After 16 days of treatment, mice were killed and tumors were excised. As mentioned earlier, H&E and IHC staining were performed on tumor tissues. The shRNA sequences used in our study were provided in the **Supplementary Table 3**.

Statistical Analysis

All experimental data analyses were carried out using Student's t -test and one-way ANOVA (GraphPad Prism 8). All data were presented as mean \pm SD. The clinical correlations between two genes were analyzed by linear regression. The interrelation between the expression of ASNR and the clinical features in GC was confirmed by Fisher's exact test. Impact of variables on survival was evaluated by univariate and multivariate Cox proportional hazard models. Overall survival (OS) rates were determined via Kaplan–Meier method. $P < 0.05$ was regarded as statistical significance.

RESULTS

Lnc_ASNR Is Highly Expressed in GC and High Level of Lnc_ASNR Predicts Poor Prognosis

Lnc_ASNR was highly expressed in the GC tissues by analyzing their expression level in the TCGA datasets and GTEx datasets through using GEPIA2 online web tool¹(**Figure 1A**). To

¹<http://gepia2.cancer-pku.cn/>

determine Lnc_ASNR expression in GC tissues, real-time PCR was carried out in GC tissues and adjacent normal tissues. The result exhibited that Lnc_ASNR expression was obviously increased in GC tissue (**Figure 1B**). Those results together indicated that Lnc_ASNR was highly expressed in GC tissue. In addition, we also measured Lnc_ASNR expression in GES-1, MKN28, AGS, MKN45, and HGC27 cells. As shown in **Figure 1E**, Lnc_ASNR expression in the GC cell lines was obviously higher than that in the GES-1 cell. Compared with the highly differentiated cell line MKN28, the Lnc_ASNR expression was higher in the lowly differentiated cell line MKN45 (**Figure 1E**).

To evaluate the clinical significance of Lnc_ASNR overexpression in GC, we explored the expression of Lnc_ASNR in 76 patients with GC and evaluated their relationship with clinicopathological features. Median expression level was considered to be the key value. Tissues were grouped into low expression group with 36 samples and high expression group with 40 samples. As indicated in **Table 1**, high Lnc_ASNR levels was significantly associated with larger tumor size ($p = 0.012$), depth of invasion ($p = 0.008$), lymph node metastasis ($p = 0.001$), and TNM stage ($p = 0.018$). In contrast, no obvious association was found between Lnc_ASNR expression and other features including gender ($p = 0.921$) and age ($p = 0.235$). Correlation between Lnc_ASNR expression level and prognosis of GC patients was evaluated. According to the upper and lower quartiles of Lnc_ASNR expression, patients are divided into high-expression and low-expression groups. It was found that the expression of Lnc_ASNR affected the survival rate of the patient using GEPIA2 web tool. The overall survival (OS) and disease-free survival (DFS) of the low ASNR group were better than the high ASNR group (**Figure 1C**). It could be confirmed from Kaplan–Meier survival analysis that Lnc_ASNR highly expressed patients exhibited shorter OS, compared with Lnc_ASNR lowly expressed patients (**Figure 1D**). In addition, univariate survival analysis showed OS of patients were significantly correlated with that tumor size, infiltrating depth, Lauren classification, tissue differentiation, TNM stage, and Lnc_ASNR expression levels (**Table 2**). These factors were further evaluated by multifactor Cox regression analysis, indicating that Lnc_ASNR expression level and tissue differentiation are independent prognostic factors for patients (**Table 3**).

Knockdown of Lnc_ASNR Inhibits While ASNR Overexpression Promotes GC Cell Proliferation, Migration, and Invasion

We hypothesized that Lnc_ASNR may act as an oncogene, based on the increased expression of Lnc_ASNR in GC. Therefore, siRNA was used to downregulate the expression of Lnc_ASNR in MKN45 cells. qRT-PCR was used to verify knockdown efficiency of siRNA, and siRNA3 was chosen for subsequent experiments because of the highest knockdown efficiency (**Figure 2A**). Cell proliferation assay (MTT) results showed that silencing Lnc_ASNR inhibited the proliferation of GC cells (**Figure 2B**). It could be seen from the flow cytometry analysis that when Lnc_ASNR was silenced, the percentage of cells in G0/G1 phase would increase, while the percentage of cells in S phase would

decrease (**Figure 2D**). The wound-healing assay and Transwell assay data suggested that compared with the control group, the si-Lnc_ASNR group significantly reduced the number of cells that migrated and invaded (**Figure 2E**).

To deeply verify whether Lnc_ASNR is related to GC, the expression of related mRNA and protein was evaluated by performing qRT-PCR and Western blot experiments. We found that both the mRNA and protein expression of PCNA, cell proliferation marker gene, was decreased (**Figure 2C**). Both mRNA and protein expression levels of cyclin A, cyclin D1, and cyclin E were decreased, while P21 and P27 expression levels were increased in the cells transfected with siRNA (**Figure 2F**). Furthermore, the mRNA and protein expression levels of MMP2, MMP9, and ICAM1, cell invasion- and migration-related gene, were decreased, while TIMP1, TIMP2, and NM23 were increased (**Figure 2F**).

Contrary to the results of silencing Lnc_ASNR, overexpression of Lnc_ASNR facilitated the proliferation, migration, and invasion of MKN28 cells (**Figures 3A–F**).

Lnc_ASNR Influences GC Cell EMT

We found that cell migration and invasion are closely related to Lnc_ASNR levels. Since epithelial-mesenchymal transition (EMT) is a key step that contributes to tumor metastasis, we evaluated the effect of Lnc_ASNR on EMT. In order to further verify the abovementioned results, qRT-PCR and Western blot assay were conducted to evaluate the EMT-induced marker expression in cells downregulating or upregulating Lnc_ASNR. As shown in **Figure 2F**, high expressed epithelial markers E-cadherin, low expressed interstitial markers N-cadherin and vimentin were detected in the cells downregulated by Lnc_ASNR, indicating that the inhibition of Lnc_ASNR promoted the change of EMT to MET. Moreover, EMT transcription factor expression, including Snail, Twist, and ZEB1, was significantly downregulated (**Figure 2F**) in si-Lnc_ASNR-transfected cells. However, the results observed in the cells transfected with pcDNA3.1-Lnc_ASNR were just the opposite (**Figure 3F**). These results are consistent with our hypothesis that Lnc_ASNR affects the malignant phenotype by regulating EMT.

Lnc_ASNR Promotes GC Cell Tumorigenesis *in vivo*

In order to provide further evidence for the above findings, stably expressed sh-Lnc_ASNR or sh-NC AGS cells were constructed by infecting cells with shRNA vectors. Then, in order to determine the correlation between Lnc_ASNR and tumorigenesis of GC cells *in vivo*, AGS cells with stable knockdown of Lnc_ASNR were injected into nude mice. In contrary to the tumor formed by the control cells, the tumor formed by the Lnc_ASNR-silenced cells has taken significantly slower time (**Figure 4A**). In addition, compared with the control group, tumor volume of the sh-Lnc_ASNR group was significantly decreased (**Figures 4B,C**). We also found that the protein expression of cell proliferation marker gene, PCNA, and cell invasion and migration-related gene, MMP2, MMP9, and ICAM1, were decreased, while NM23 was increased

TABLE 1 | Association of Lnc_ASNR expression with clinicopathological features of gastric cancer.

Features	Number	Lnc_ASNR expression levels		χ^2	p-Value
		High	Low		
Gender					
Male	46	24	22	0.010	0.921
Female	30	16	14		
Age (years)					
≤59	35	21	14	1.413	0.235
>59	41	19	22		
Tumor size (cm)					
≤4.8	48	20	28	6.283	0.012
>4.8	28	20	8		
Lauren classification					
Intestinal	21	7	14	11.689	0.003
Diffuse	30	23	7		
Mixed	25	10	15		
Tissue differentiation					
Well	5	0	5	12.110	0.001
Moderate	36	15	21		
Poor	35	25	10		
Infiltrating depth					
T1	3	0	3	10.717	0.008
T2	26	9	17		
T3	40	25	15		
T4	7	6	1		
Nodal status					
N0	18	3	15	16.223	0.001
N1	16	8	8		
N2	18	10	8		
N3	25	19	5		
Distant metastasis					
M0	74	38	36	1.849	0.495
M1	2	2	0		
TNM stage					
I	6	1	5	8.756	0.018
II	28	11	17		
III	40	26	14		
IV	2	2	0		

in the sh-Lnc_ASNR group (**Figure 4D**). The above results demonstrated that the downregulated Lnc_ASNR could suppress tumor development *in vivo*. Furthermore, the results of H&E staining indicated that the sh-Lnc_ASNR group significantly suppressed tumorigenesis. Additionally, immunohistochemical staining of tumor tissues demonstrated that contrary to the sh-NC group, a decrease in Ki-67 was detected in the sh-Lnc_ASNR group (**Figure 4E**).

In vivo investigations above complement the evidence of *in vitro* functional studies involving Lnc_ASNR.

Lnc_ASNR Functions as ceRNA and Sponges miR-519e-5p in GC Cells

In addition to regulating the target in epigenetics, some lncRNAs can also act as competing endogenous RNA (ceRNA) of specific

miRNA to affect the target gene expression. We predicted the potential target of Lnc_ASNR by searching the biological information database miRDB. We examined the Lnc_ASNR sequence and found the miR-519e-5p-binding site and identified miR-519e-5p as a candidate binding miRNA (**Figure 5A**). In order to detect the miR-519e-5p expression in GC tissues, real-time PCR was performed in GC tissues and matched adjacent normal tissues. It was clearly indicated that the expression of miR-519e-5p was markedly downregulated in GC samples (**Figure 5B**). Besides, Lnc_ASNR expression was negatively correlated with that of miR-519e-5p in GC samples (**Figure 5C**). We attempted to analyze the regulation of miR-519e-5p by Lnc_ASNR. Highly differentiated MKN28 cells were transfected pcDNA3.1(+) vector carrying the coding sequence of Lnc_ASNR to overexpress Lnc_ASNR, and downregulation of miR-519e-5p

TABLE 2 | Univariate analysis of prognostic factors in 76 patients with gastric cancer.

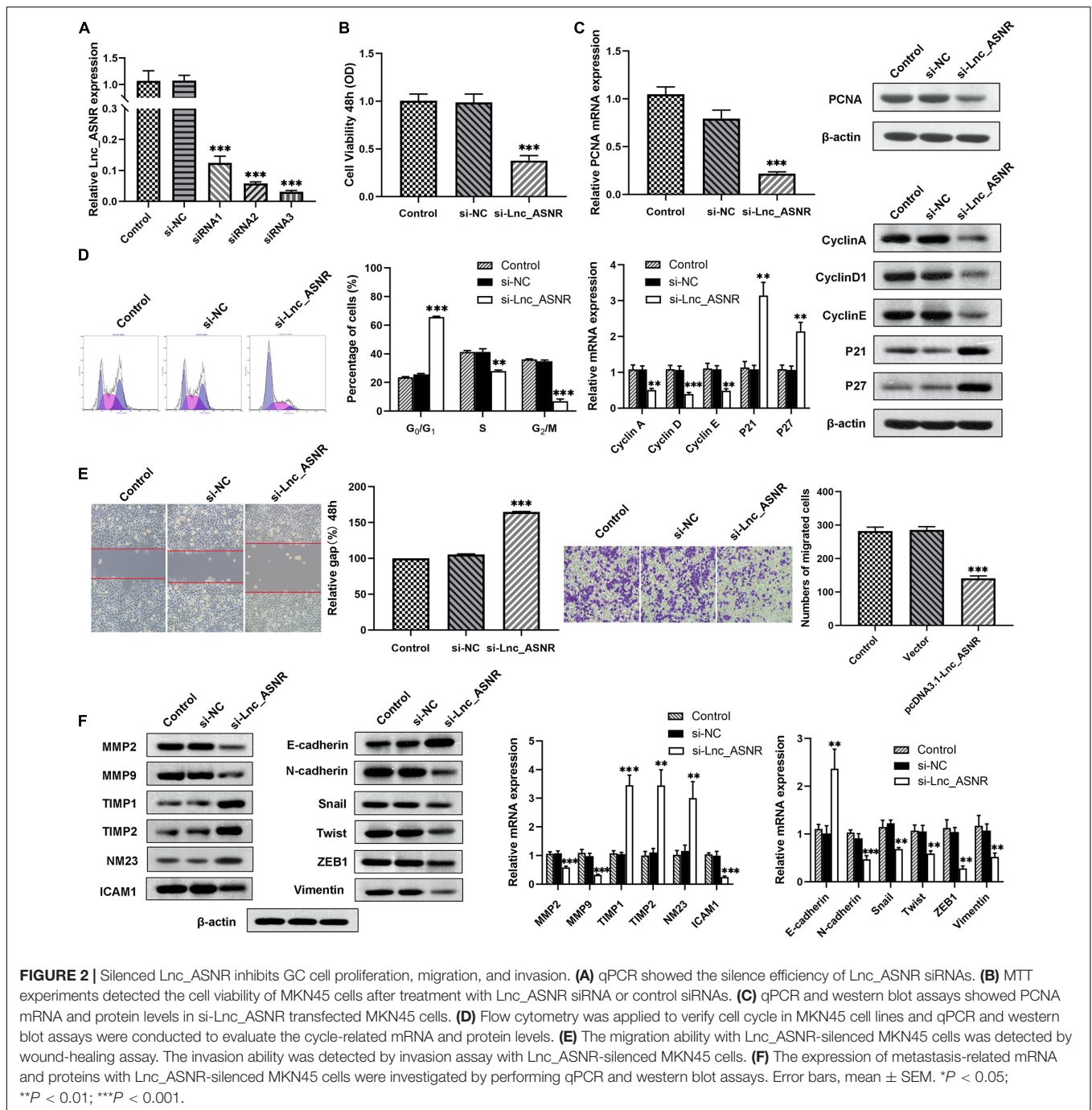
Characteristics	All cases	5-year survival rate	χ^2	p-Value
Gender				
Male	46	54.35% (25/46)	0.039	0.842
Female	30	56.67% (17/30)		
Age (years)				
<60	35	54.29% (19/35)	0.025	0.874
≥60	41	56.10% (23/41)		
Tumor size (cm)				
≤4.8	48	66.67% (32/48)	6.853	0.009
>4.8	28	35.71% (10/28)		
Lauren classification				
Intestinal	21	76.19% (16/21)	8.143	0.017
Diffuse	30	36.67% (11/30)		
Mixed	25	60.00% (15/25)		
Tissue differentiation				
Well	5	100.00% (5/5)	6.521	0.037
Moderate	36	61.11% (22/36)		
Poor	35	42.86% (15/35)		
Infiltrating depth				
T1	3	100.00% (3/3)	9.041	0.019
T2	26	69.23% (18/26)		
T3	40	50.00% (20/40)		
T4	7	14.29% (1/7)		
Nodal status				
N0	18	72.22% (13/18)	3.208	0.361
N1	16	50.00% (8/16)		
N2	18	44.44% (8/18)		
N3	25	52.00% (13/25)		
Distant metastasis				
M0	74	56.76% (42/74)	2.537	0.197
M1	2	0.00% (0/2)		
TNM stage				
I	6	83.33% (5/6)	7.253	0.041
II	28	67.86% (19/28)		
III	40	45.00% (18/40)		
IV	2	0.00% (0/2)		
ASNR expression				
Low	36	75.00% (27/36)	10.777	0.001
High	40	37.50% (15/40)		

TABLE 3 | Multivariate analysis of prognostic factors in 76 patients with gastric cancer.

Clinicopathological features	B	SE	Wald	p-Value	95% CI
Tumor size (cm)	0.350	0.515	0.462	0.497	0.257~1.934
Lauren classification	1.974	1.185	2.775	0.096	0.706~73.446
Tissue differentiation	3.301	1.228	7.228	0.007	2.446~300.984
Infiltrating depth	0.104	0.739	0.020	0.888	0.261~4.724
TNM stage	1.789	1.246	2.062	0.151	0.520~68.760
ASNR expression	2.772	0.821	11.400	0.001	0.013~0.313

expression was detected by qPCR (**Figure 5D**). Whereas, lowly differentiated MKN45 cells were transfected with si-Lnc_ASNR to silence Lnc_ASNR and upregulated miR-519e-5p expression

was detected by qPCR (**Figure 5E**). To further verify the targeting relationships between miR-519e-5p and Lnc_ASNR, luciferase reporter experiment was performed in MKN45 cells.



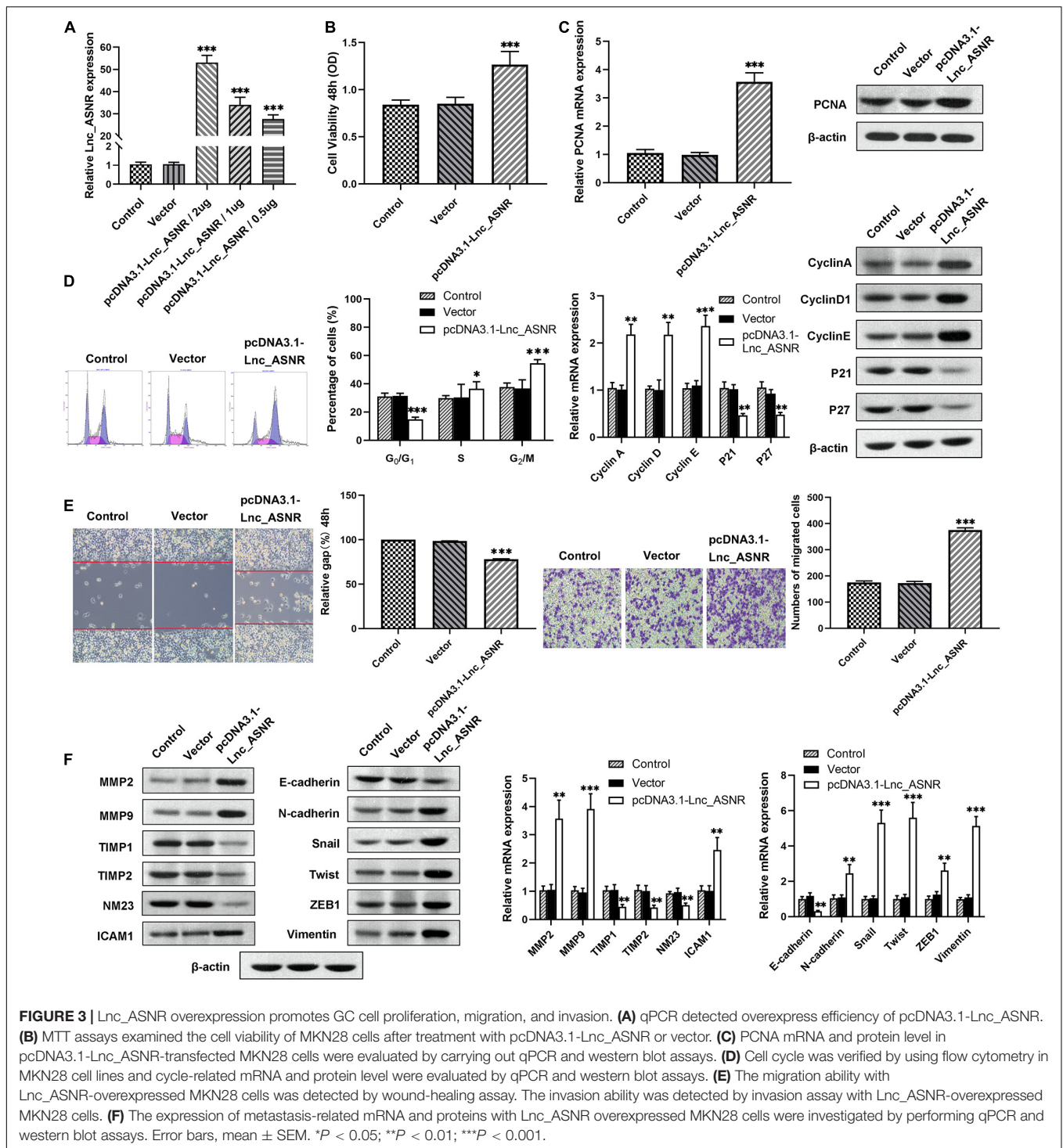
As represented in **Figure 5F**, miR-519e-5p mimic apparently decreased the activity of luciferase in Lnc_ASNR-wild, while no significant change was detected in Lnc_ASNR-mut.

Therefore, these data suggested that Lnc_ASNR acts as a miR-519e-5p sponge in GC.

FGFR2 Is a Downstream Target of miR-519e-5p

Online miRNA target prediction databases (including Targetscan and miRDB) were applied to predict potential target genes

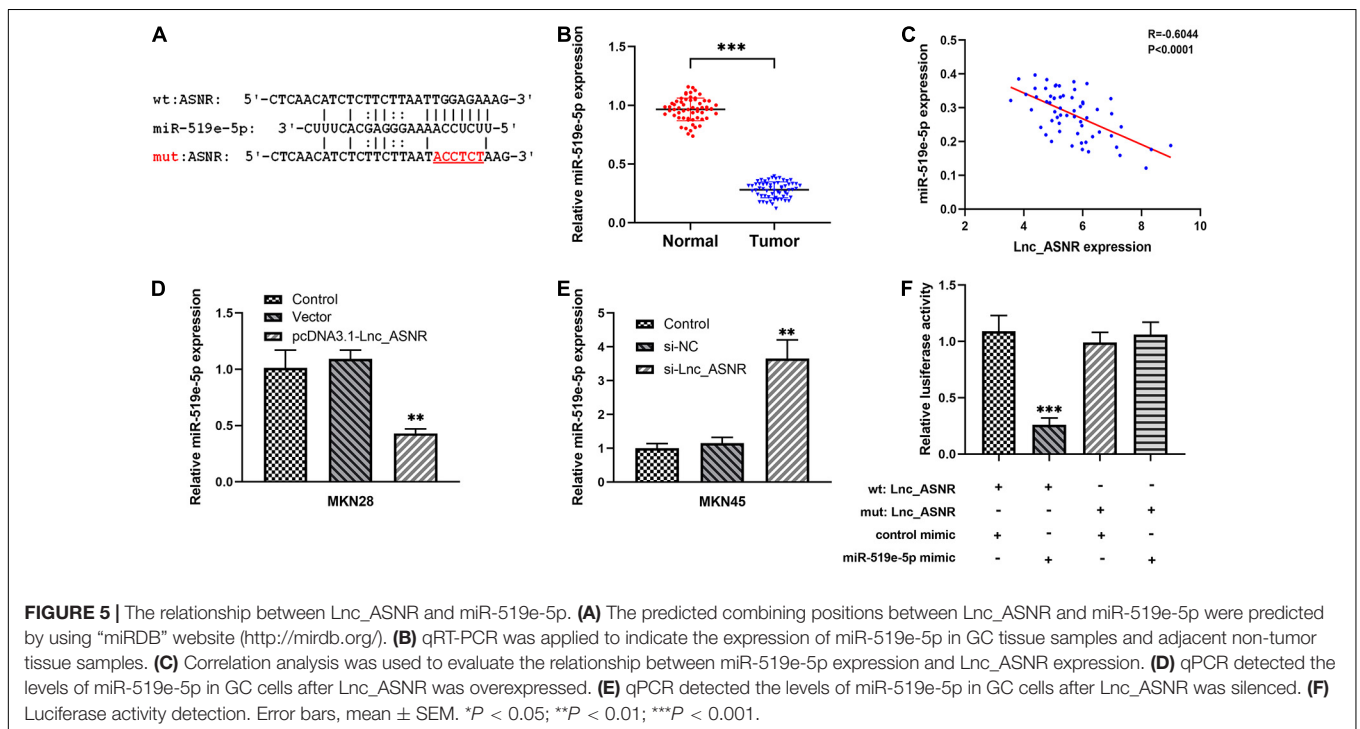
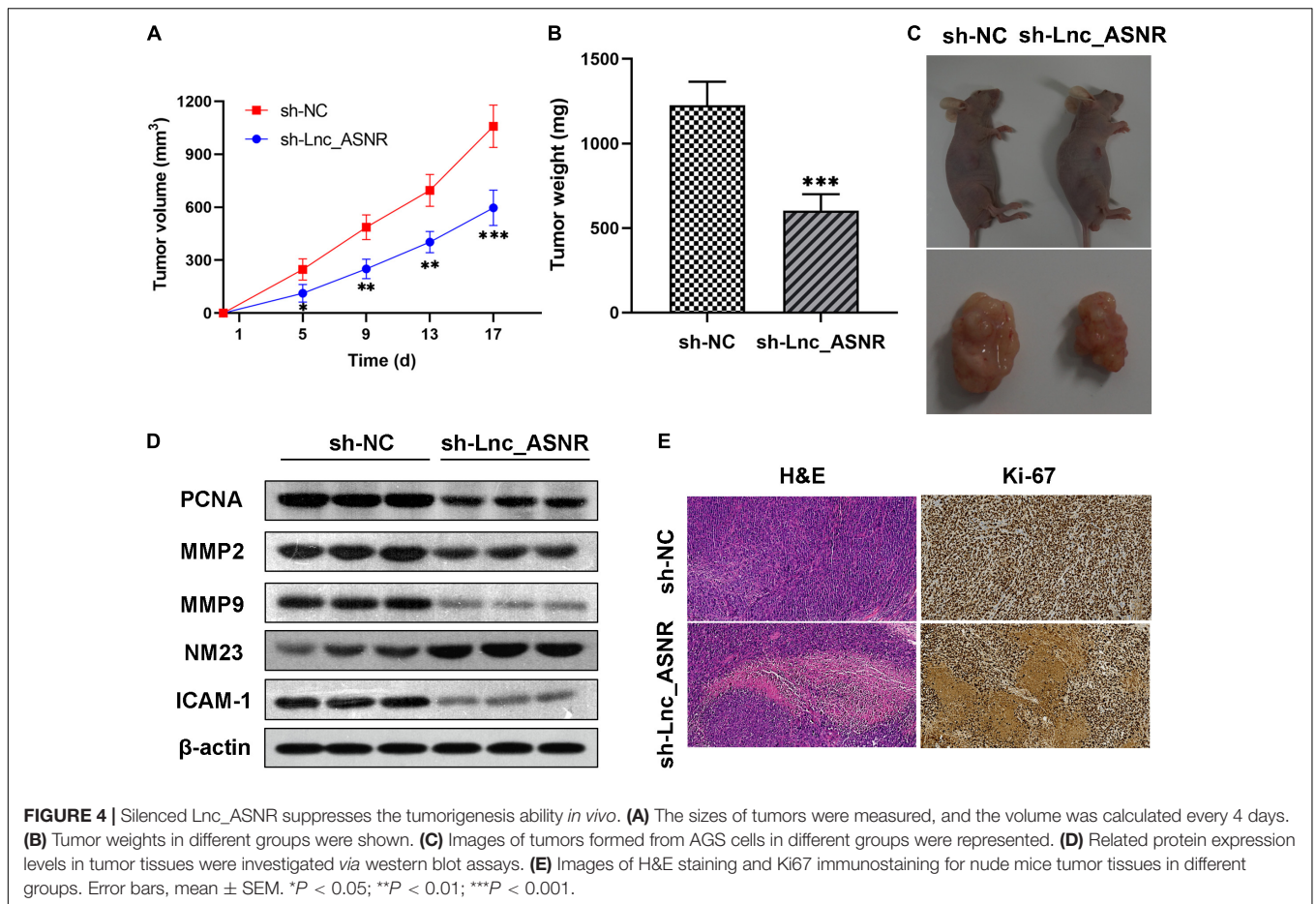
of miR-519e-5p, and FGFR2 was determined as a potential downstream gene of miR-519e-5p (**Figure 6A**). Real-time PCR was carried out in GC tissues and matched adjacent normal tissues to evaluate the FGFR2 expression. An obvious upregulation of FGFR2 expression was detected in GC tissue samples (**Figure 6B**). Besides, FGFR2 expression was positively correlated with the expression of Lnc_ASNR (**Figure 6C**) and negatively related to miR-519e-5p expression in GC tissue samples (**Figure 6D**). In addition, FGFR2 expression in GES-1, MKN28, AGS, MKN45, and HGC27 cells was also detected. It



was clearly indicated from **Figure 6E** that FGFR2 expression was markedly higher in GC cell lines than that of control cells.

Next, low differentiated MKN45 cells were transfected with miR-519e-5p mimic, and qRT-PCR was used to verify that miR-519e-5p expression was markedly increased (**Figure 6F**). In addition, the FGFR2 expression level was evaluated by qRT-PCR and Western blot experiments, and the data demonstrated

that the FGFR2 expression level was markedly downregulated (**Figure 6G**). On the contrary, miR-519e-5p inhibitor was used to transfected highly differentiated MKN28 cells, and corresponding results demonstrated that the expression of miR-519e-5p was markedly decreased (**Figure 6H**). Moreover, FGFR2 expression was investigated by conducting qRT-PCR and Western blot experiments, and the results suggested that FGFR2 expression



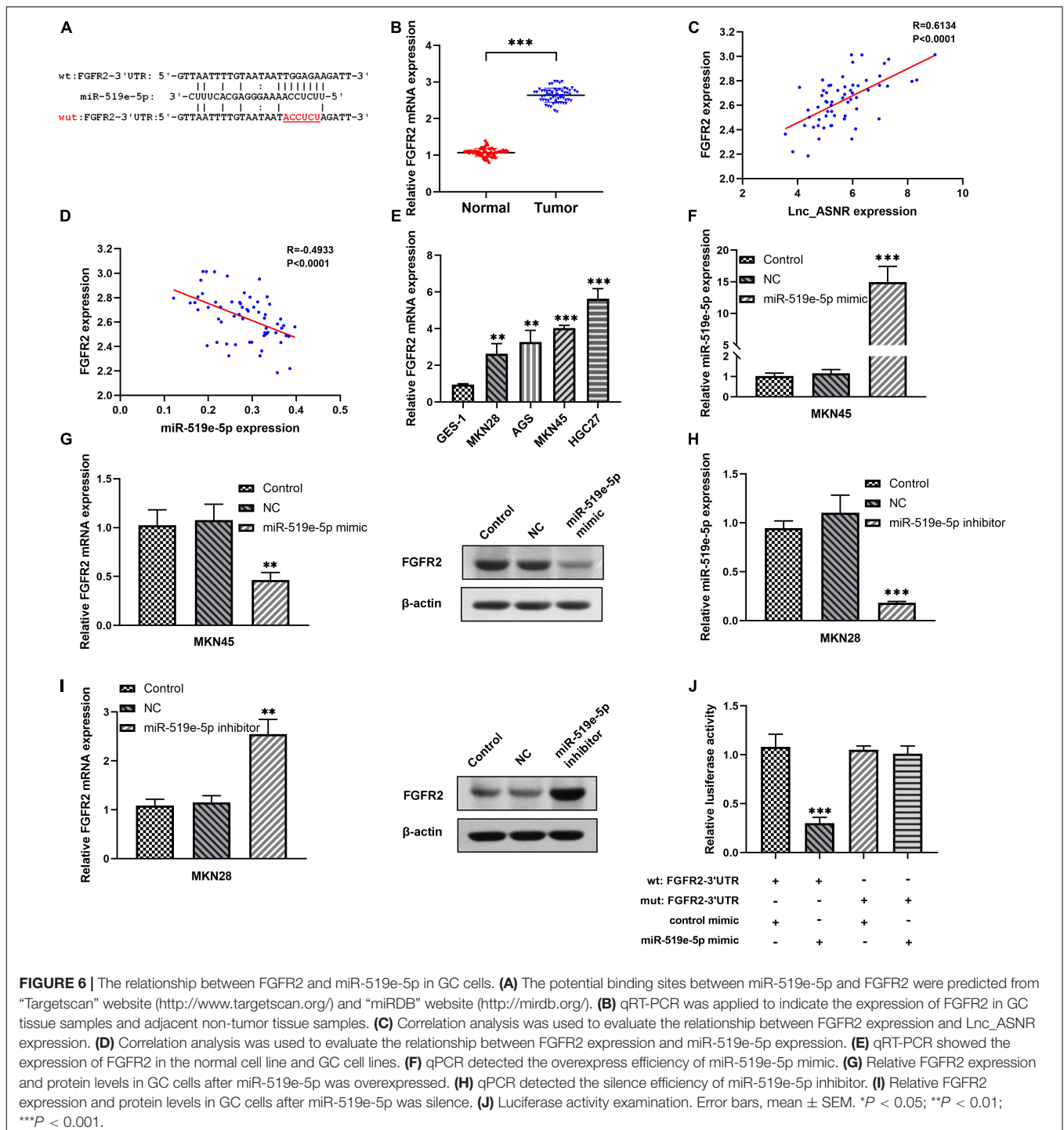


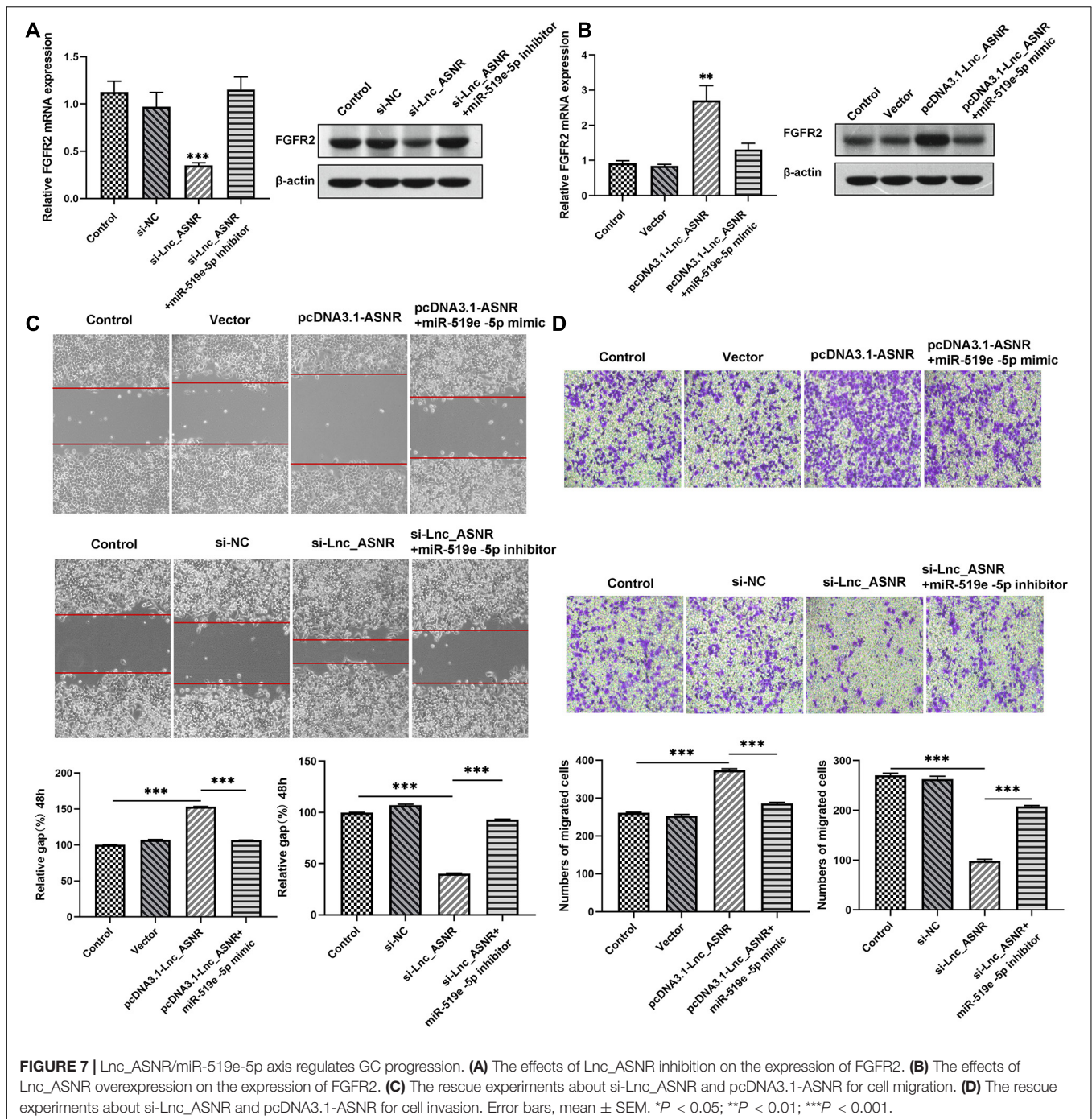
FIGURE 6 | The relationship between FGFR2 and miR-519e-5p in GC cells. **(A)** The potential binding sites between miR-519e-5p and FGFR2 were predicted from “Targetscan” website (<http://www.targetscan.org/>) and “miRDB” website (<http://mirdb.org/>). **(B)** qRT-PCR was applied to indicate the expression of FGFR2 in GC tissue samples and adjacent non-tumor tissue samples. **(C)** Correlation analysis was used to evaluate the relationship between FGFR2 expression and Lnc_ASNR expression. **(D)** Correlation analysis was used to evaluate the relationship between FGFR2 expression and miR-519e-5p expression. **(E)** qRT-PCR showed the expression of FGFR2 in the normal cell line and GC cell lines. **(F)** qPCR detected the overexpress efficiency of miR-519e-5p mimic. **(G)** Relative FGFR2 expression and protein levels in GC cells after miR-519e-5p was overexpressed. **(H)** qPCR detected the silence efficiency of miR-519e-5p inhibitor. **(I)** Relative FGFR2 expression and protein levels in GC cells after miR-519e-5p was silence. **(J)** Luciferase activity examination. Error bars, mean \pm SEM. * $P < 0.05$; ** $P < 0.01$; *** $P < 0.001$.

was obviously increased (Figure 6I). To further evaluate the targeting correlation between miR-519e-5p and FGFR2, luciferase reporter experiment was performed in the MKN45 cells. As exhibited in Figure 6J, miR-519e-5p mimic markedly suppressed the vitality of luciferase in FGFR2-wild, while no significant change was detected in FGFR2-mut.

Therefore, these data indicated that FGFR2 is an important downstream target of miR-519e-5p.

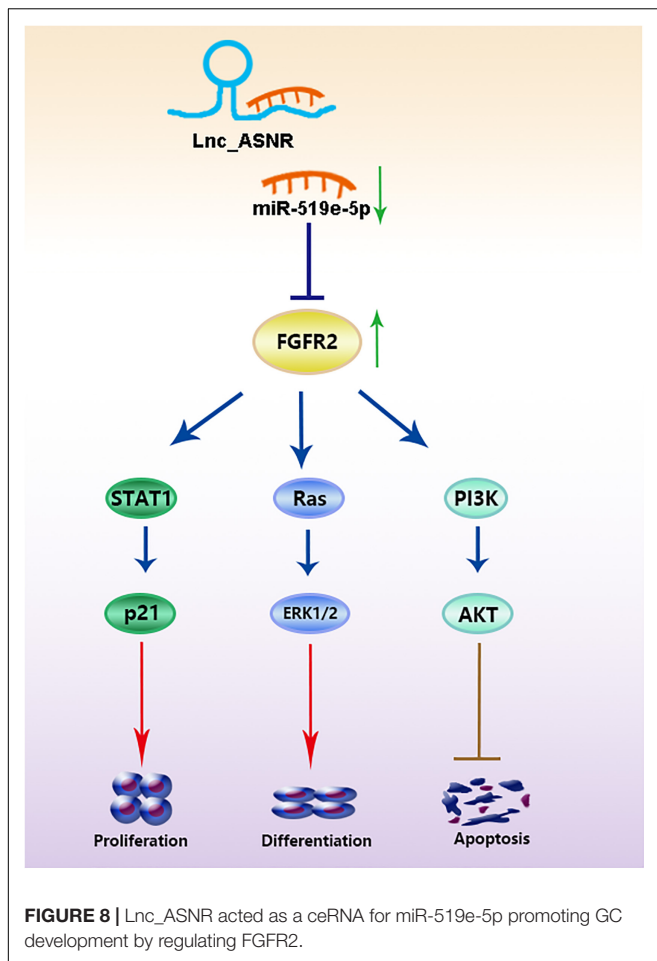
The Lnc_ASNR/miR-519e-5p/FGFR2 Axis Promotes Proliferation, Invasion, and Migration of GC

Mechanism research was conducted to clarify the relationship between Lnc_ASNR and FGFR2. Lnc_ASNR was silenced in lowly differentiated MKN45 cells. qRT-PCR and western blot assay inhibited that decreased Lnc_ASNR reduced the level



of FGFR2 protein, which is consistent with the miR-519e-5p-induced FGFR2 protein downregulation. When transfected with si-ASNR + miR-519e-5p inhibitor in MKN45 cells, it was found that FGFR2 expression was restored (**Figure 7A**). In contrast, upregulated FGFR2 was detected in highly differentiated MKN28 cells who overexpressed Lnc_ASNR. When pcDNA3.1-ASNR + miR-519e-5p mimic was transfected in MKN45 cells, it was found that FGFR2 expression was reversed (**Figure 7B**). The effect of Lnc_ASNR/miR-519e-5p axis on GC

was then evaluated. MKN28 cells were transfected with vectors, pcDNA3.1-ASNR, and pcDNA3.1-ASNR + miR-519e-5p mimic, respectively. MKN45 cells were transfected with si-NC, si-ASNR, and si-ASNR + miR-519e-5p inhibitors, respectively. As shown in **Figures 7C,D**, miR-519e-5p mimics could counteract the enhancement effect of overexpression of Lnc_ASNR on cell migration and invasion ability, while miR-519e-5p inhibitor could reverse the inhibitory effect of knockdown of Lnc_ASNR on cell migration and invasion ability.



Ultimately, correlation analysis in GC showed that Lnc_ASNR expression and miR-519e-5p expression was negatively related, while Lnc_ASNR expression and FGFR2 expression was positively related. Overall, the above results demonstrated that Lnc_ASNR acted as a ceRNA for miR-519e-5p, thereby reducing FGFR2 expression and imposing posttranscriptional regulatory levels (Figure 8).

DISCUSSION

Generally, explorations for cancer drivers are focused on protein-coding genes in cancer genomes before the discovery of non-coding RNAs. However, increasing research results verified that lncRNAs are crucial in cellular progression and diseases development (Han et al., 2019; Pradas-Juni et al., 2020), especially in cancer (Papaioannou et al., 2019; Schulte et al., 2020; Silva-Fisher et al., 2020). Abnormal expression of lncRNAs may lead to accelerated tumor growth (Geng et al., 2018; Lin and Yang, 2018; Sallam et al., 2018). The therapeutic methods available to advanced GC patients are limited, and there remains potential to improve the treatment effect. It is essential to investigate

thoroughly the internal mechanisms of GC occurrence and development and explore novel prognostic markers. Large amounts of lncRNAs are verified to play crucial roles in GC development. Increasing researchers pay more attention to investigate the functions and regulation of lncRNAs to explore novel predictors for the diagnosis and therapeutics of GC (Fu et al., 2020; Qin et al., 2020; Ren et al., 2020). Herein, a GC-associated lncRNA ASNR was identified, which was markedly increased in GC cells and tissues. High Lnc_ASNR expression was related to advanced TNM staging, larger tumor size, and positive lymph node metastasis. In addition, the upregulated expression of Lnc_ASNR was related to the shortening of OS and DFS in GC patients. The above investigations showed that knocking down Lnc_ASNR suppressed cell proliferation, declined tumor growth, and facilitated cell apoptosis, while upregulated Lnc_ASNR accelerated cell proliferation, invasion, and metastasis. These functional evidences indicate that Lnc_ASNR plays a carcinogenic role in the occurrence of GC, which can be used as a potential prognostic indicator.

Increasing evidences indicate that there is a novel and extensive interaction network involving ceRNA. It was reported that ncRNAs could regulate target RNA through combining their linking position of protein coding messengers (Wang P. et al., 2020; Wang W. et al., 2020; Zhao et al., 2020). Emerging researches confirm the ceRNA hypothesis and indicate that ceRNA regulation is related to the carcinogenic effects of GC. For example, lncRNA MT1JP can suppress cell growth, migration, and invasion, promote cell apoptosis *in vitro*, and inhibit tumor growth and metastasis *in vivo* (Zhang et al., 2018). In our previous investigations, we suggested that lncRNA PWRN1 acts as a ceRNA-targeting miR-425-5p and inhibits the growth of GC by intervening p53 signaling pathway (Chen et al., 2018). Thus, we assumed that lncRNA may play the role of ceRNA and participate in occurrence of GC. It was confirmed by bioinformatics analysis and luciferase reporter gene analysis that miR-519e-5p was targeted by Lnc_ASNR. Recently, miR-519e-5p has only been reported in acute myocardial infarction (Wang F. et al., 2014) and pregnancy-related complications (Hromadnikova et al., 2015; Zhang et al., 2016), while few investigations on the relationship between miR-519e-5p and GC were reported. In our research, we confirmed that the endogenous level of Lnc_ASNR could influence the miR-519e-5p expression. The miR-519e-5p expression was increased in GC cells when Lnc_ASNR was silenced. Contrary to the results of silencing Lnc_ASNR, miR-519e-5p expression was decreased upon Lnc_ASNR overexpression, which confirmed our hypothesis. Above investigations revealed the importance of the correlation between Lnc_ASNR with miR-519e-5p in GC, which was contributed to that Lnc_ASNR exhibited a carcinogenic effect through causing miR-519e-5p to produce sponges in GC cells.

In general, lncRNAs exhibit function by relying on ceRNA to inhibit miRNA targets (Shen et al., 2018; Chen et al., 2019; Yang et al., 2019). Therefore, miRNA targets are important

parts of ceRNA network. It is worth to note that FGFR2 is a potential miR-519e-5p target site which has never been reported *via* online-predicting database. In order to verify that miR-519e-5p was directly targeted by FGFR2, we carried out luciferase reporter experiments and confirmed that FGFR2 was targeted by miR-519e-5p at 3'-UTR. In addition, transfection of miR-519e-5p mimic inhibits FGFR2 mRNA and protein expression, while transfection of miR-519e-5p inhibitor promotes FGFR2 mRNA and protein expression. The protein encoded by the FGFR2 gene is one of the members of the fibroblast growth factor receptor (FGFR) family (Wu et al., 2013). At present, four types of FGFRs have been identified, namely FGFR1, FGFR2, FGFR3, and FGFR4. The main function of FGFR, a receptor for FGF, is to transduce FGF signal to RAS-ERK and PI3K-AKT signal cascade amplification. The missense mutations of the FGFR2 gene occur in endometrial cancer, cervical cancer, breast cancer, lung cancer, and GC. The amplified FGFR2 induces the activation of FGFR2 signaling. FGFR2 has been proposed as a target for targeted therapy of GC (Pearson et al., 2016; Kuboki et al., 2018; Kim et al., 2019). Yu et al. (2018) revealed that overexpressed FGFR2 accelerated the production of cancer-initiating cells (CIC) and enhanced the resistance to lapatinib in HER2-positive GC cells. We further determined that miR-519e-5p could reverse the effect of Lnc_ASNR on FGFR2 expression level, indicating that Lnc_ASNR acts on miR-519e-5p through sponge adsorption, which further affects the expression of downstream target gene FGFR2, thereby affecting cell proliferation, invasion, and migration activity.

In summary, our findings validated a novel lncRNA, called Lnc_ASNR, and found that Lnc_ASNR expression was related to poor prognosis in GC. The study found that Lnc_ASNR was a carcinogenic lncRNA exhibiting a targeting relationship with miR-519e-5p. GC patients with higher expression of Lnc_ASNR promoted tumor growth by regulating the miR-519e-5p/FGFR2 pathway. The current study reveals a further insight into the function of lncRNA-miRNA-mRNA-ceRNA network in GC progression. The promoter function of Lnc_ASNR in the GC progress was first reported. The potential molecular mechanism involved in the Lnc_ASNR/miR-519e-5p/FGFR2 axis could be a potentially useful approach for GC diagnosis and therapies.

REFERENCES

- Bray, F., Ferlay, J., Soerjomataram, I., Siegel, R. L., Torre, L. A., and Jemal, A. (2018). Global cancer statistics 2018: GLOBOCAN estimates of incidence and mortality worldwide for 36 cancers in 185 countries. *CA Cancer J. Clin.* 68, 394–424. doi: 10.3322/caac.21492
- Chen, J., Liu, L., Wei, G., Wu, W., Luo, H., Yuan, J., et al. (2016). The long noncoding RNA ASNR regulates degradation of Bcl-2 mRNA through its interaction with AUF1. *Sci. Rep.* 6:32189. doi: 10.1038/srep32189
- Chen, J., Yu, Y., Li, H., Hu, Q., Chen, X., He, Y., et al. (2019). Long non-coding RNA PVT1 promotes tumor progression by regulating the miR-143/HK2 axis in gallbladder cancer. *Mol. Cancer* 18:33. doi: 10.1186/s12943-019-0947-9
- Chen, Z., Ju, H., Yu, S., Zhao, T., Jing, X., Li, P., et al. (2018). Prader-Willi region non-protein coding RNA 1 suppressed gastric cancer growth as a competing

DATA AVAILABILITY STATEMENT

The original contributions presented in the study are included in the article/**Supplementary Material**, further inquiries can be directed to the corresponding author/s.

ETHICS STATEMENT

The animal study was reviewed and approved by Research Ethics Committee at the Fourth Hospital of Hebei Medical University. Written informed consent was obtained from the individual(s) for the publication of any potentially identifiable images or data included in this article.

AUTHOR CONTRIBUTIONS

ZC and YLo planned, designed, and coordinated this research and drafted the manuscript. BT and QZ participated in the conception and design of the manuscript and revised it critically for important intellectual content. FL and LF contributed to the conception and design and helped in drafting the manuscript. ZZ, XZ, and YLu contributed to analyzing and interpreting data and improved the crucial parts. DW helped in writing a part of the manuscript and analyzed the data. All the authors read and approved the final manuscript.

ACKNOWLEDGMENTS

We thank all the members in our laboratory and department and all the patients and their families involved in the current study.

SUPPLEMENTARY MATERIAL

The Supplementary Material for this article can be found online at: <https://www.frontiersin.org/articles/10.3389/fcell.2021.679176/full#supplementary-material>

- endogenous RNA of miR-425-5p. *Clin. Sci.* 132, 1003–1019. doi: 10.1042/CS20171588
- den Hollander, W. J., Holster, I. L., den Hoed, C. M., Capelle, L. G., Tang, T. J., Anten, M. P., et al. (2019). Surveillance of premalignant gastric lesions: a multicentre prospective cohort study from low incidence regions. *Gut* 68, 585–593. doi: 10.1136/gutjnl-2017-314498
- Fu, T., Ji, K., Jin, L., Zhang, J., Wu, X., Ji, X., et al. (2020). ASB16-AS1 up-regulated and phosphorylated TRIM37 to activate NF-kappaB pathway and promote proliferation, stemness, and cisplatin resistance of gastric cancer. *Gastric Cancer* 24, 45–59. doi: 10.1007/s10120-020-01096-y
- Geng, H., Bu, H. F., Liu, F., Wu, L., Pfeifer, K., Chou, P. M., et al. (2018). In inflamed intestinal tissues and epithelial cells, interleukin 22 signaling increases expression of H19 long noncoding RNA, which promotes mucosal regeneration. *Gastroenterology* 155, 144–155. doi: 10.1053/j.gastro.2018.03.058

- Guo, X., Lv, X., Ru, Y., Zhou, F., Wang, N., Xi, H., et al. (2020). Circulating exosomal gastric cancer-associated long noncoding RNA1 as a biomarker for early detection and monitoring progression of gastric cancer: a multiphase study. *JAMA Surg.* 155, 572–579. doi: 10.1001/jamasurg.2020.1133
- Han, X., Huang, S., Xue, P., Fu, J., Liu, L., Zhang, C., et al. (2019). LncRNA PTPRE-AS1 modulates M2 macrophage activation and inflammatory diseases by epigenetic promotion of PTPRE. *Sci. Adv.* 5:eaa9230. doi: 10.1126/sciadv.aax9230
- Hromadnikova, I., Kotlabova, K., Ondrackova, M., Pirkova, P., Kestlerova, A., Novotna, V., et al. (2015). Expression profile of C19MC microRNAs in placental tissue in pregnancy-related complications. *DNA Cell Biol.* 34, 437–457. doi: 10.1089/dna.2014.2687
- Huang, Y., Xu, Y., Lu, Y., Zhu, S., Guo, Y., Sun, C., et al. (2019). LncRNA Gm10451 regulates PTPIP to facilitate iPSCs-derived beta-like cell differentiation by targeting miR-338-3p as a ceRNA. *Biomaterials* 216:119266. doi: 10.1016/j.biomaterials.2019.119266
- Kim, H. S., Kim, J. H., and Jang, H. J. (2019). Pathologic and prognostic impacts of FGFR2 amplification in gastric cancer: a meta-analysis and systemic review. *J. Cancer* 10, 2560–2567. doi: 10.7150/jca.29184
- Kim, J., Piao, H. L., Kim, B. J., Yao, F., Han, Z., Wang, Y., et al. (2018). Long noncoding RNA MALAT1 suppresses breast cancer metastasis. *Nat. Genet.* 50, 1705–1715. doi: 10.1038/s41588-018-0252-3
- Kuboki, Y., Schatz, C. A., Koechert, K., Schubert, S., Feng, J., Wittemer-Rump, S., et al. (2018). In situ analysis of FGFR2 mRNA and comparison with FGFR2 gene copy number by dual-color in situ hybridization in a large cohort of gastric cancer patients. *Gastric Cancer* 21, 401–412. doi: 10.1007/s10120-017-0758-x
- Lin, C., and Yang, L. (2018). Long noncoding RNA in cancer: wiring signaling circuitry. *Trends Cell Biol.* 28, 287–301. doi: 10.1016/j.tcb.2017.11.008
- Montes, M., Lubas, M., Arendrup, F. S., Mentz, B., Rohatgi, N., Tumas, S., et al. (2021). The long non-coding RNA MIR31HG regulates the senescence associated secretory phenotype. *Nat. Commun.* 12:2459. doi: 10.1038/s41467-021-22746-4
- Olivero, C. E., Martinez-Terroba, E., Zimmer, J., Liao, C., Tesfaye, E., Hooshdaran, N., et al. (2020). p53 activates the long noncoding RNA Pvt1b to inhibit Myc and suppress tumorigenesis. *Mol. Cell* 77, 761–774.e8. doi: 10.1016/j.molcel.2019.12.014
- Papaioannou, D., Petri, A., Dovey, O. M., Terreri, S., Wang, E., Collins, F. A., et al. (2019). The long non-coding RNA HOXB-AS3 regulates ribosomal RNA transcription in NPM1-mutated acute myeloid leukemia. *Nat. Commun.* 10:5351. doi: 10.1038/s41467-019-13259-2
- Pearson, A., Smyth, E., Babina, I. S., Herrera-Abreu, M. T., Tarazona, N., Peckitt, C., et al. (2016). High-level clonal FGFR amplification and response to FGFR inhibition in a translational clinical trial. *Cancer Discov.* 6, 838–851. doi: 10.1158/2159-8290.CD-15-1246
- Pradas-Juni, M., Hansmeier, N. R., Link, J. C., Schmidt, E., Larsen, B. D., Klemm, P., et al. (2020). A MAFG-lncRNA axis links systemic nutrient abundance to hepatic glucose metabolism. *Nat. Commun.* 11:644. doi: 10.1038/s41467-020-14323-y
- Qin, C., Jin, L., Li, J., Zha, W., Ding, H., Liu, X., et al. (2020). Long non-coding RNA LINC02163 accelerates malignant tumor behaviors in breast cancer by regulating the microRNA-511-3p/HMG2 axis. *Oncol. Res.* 28, 483–495. doi: 10.3727/096504020X15928179818438
- Ramnarine, V. R., Kobelev, M., Gibb, E. A., Nouri, M., Lin, D., Wang, Y., et al. (2019). The evolution of long noncoding RNA acceptance in prostate cancer initiation, progression, and its clinical utility in disease management. *Eur. Urol.* 76, 546–559. doi: 10.1016/j.eururo.2019.07.040
- Ren, Z., Liu, X., Si, Y., and Yang, D. (2020). Long non-coding RNA DDX11-AS1 facilitates gastric cancer progression by regulating miR-873-5p/SPC18 axis. *Artif. Cells Nanomed. Biotechnol.* 48, 572–583. doi: 10.1080/21691401.2020.1726937
- Sallam, T., Sandhu, J., and Tontonoz, P. (2018). Long noncoding RNA discovery in cardiovascular disease: decoding form to function. *Circ. Res.* 122, 155–166. doi: 10.1161/CIRCRESAHA.117.311802
- Schulte, C., Barwari, T., Joshi, A., Zeller, T., and Mayr, M. (2020). Noncoding RNAs versus protein biomarkers in cardiovascular disease. *Trends Mol. Med.* 26, 583–596. doi: 10.1016/j.molmed.2020.02.001
- Shang, Z., Yu, J., Sun, L., Tian, J., Zhu, S., Zhang, B., et al. (2019). LncRNA PCAT1 activates AKT and NF-kappaB signaling in castration-resistant prostate cancer by regulating the PHLPP/FKBP51/IKKalpha complex. *Nucleic Acids Res.* 47, 4211–4225. doi: 10.1093/nar/gkz108
- Shen, L., Wang, Q., Liu, R., Chen, Z., Zhang, X., Zhou, P., et al. (2018). LncRNA lnc-RI regulates homologous recombination repair of DNA double-strand breaks by stabilizing RAD51 mRNA as a competitive endogenous RNA. *Nucleic Acids Res.* 46, 717–729. doi: 10.1093/nar/gkx1224
- Silva-Fisher, J. M., Dang, H. X., White, N. M., Strand, M. S., Krasnick, B. A., Rozycki, E. B., et al. (2020). Long non-coding RNA RAMS11 promotes metastatic colorectal cancer progression. *Nat. Commun.* 11:2156. doi: 10.1038/s41467-020-15547-8
- Song, Y. X., Sun, J. X., Zhao, J. H., Yang, Y. C., Shi, J. X., Wu, Z. H., et al. (2017). Non-coding RNAs participate in the regulatory network of CLDN4 via ceRNA mediated miRNA evasion. *Nat. Commun.* 8:289. doi: 10.1038/s41467-017-00304-1
- Sun, Y., Zhou, Y., Bai, Y., Wang, Q., Bao, J., Luo, Y., et al. (2017). A long non-coding RNA HOTTIP expression is associated with disease progression and predicts outcome in small cell lung cancer patients. *Mol. Cancer* 16:162. doi: 10.1186/s12943-017-0729-1
- Ulitsky, I. (2016). Evolution to the rescue: using comparative genomics to understand long non-coding RNAs. *Nat. Rev. Genet.* 17, 601–614. doi: 10.1038/nrg.2016.85
- Virgilio, E., Proietti, A., D'Urso, R., Cardelli, P., Giarnieri, E., Montagnini, M., et al. (2017). Measuring intragastric tumor markers in gastric cancer patients: a systematic literature review on significance and reliability. *Anticancer Res.* 37, 2817–2821. doi: 10.21873/anticancer.11632
- Wang, C. J., Zhu, C. C., Xu, J., Wang, M., Zhao, W. Y., Liu, Q., et al. (2019). The lncRNA UCA1 promotes proliferation, migration, immune escape and inhibits apoptosis in gastric cancer by sponging anti-tumor miRNAs. *Mol. Cancer* 18:115. doi: 10.1186/s12943-019-1032-0
- Wang, F., Long, G., Zhao, C., Li, H., Chaugai, S., Wang, Y., et al. (2014). Atherosclerosis-related circulating miRNAs as novel and sensitive predictors for acute myocardial infarction. *PLoS One* 9:e105734. doi: 10.1371/journal.pone.0105734
- Wang, P., Li, X., Gao, Y., Guo, Q., Ning, S., Zhang, Y., et al. (2020). LnCeVar: a comprehensive database of genomic variations that disturb ceRNA network regulation. *Nucleic Acids Res.* 48, D111–D117. doi: 10.1093/nar/gkz887
- Wang, W., Hu, W., Wang, Y., An, Y., Song, L., Shang, P., et al. (2020). Long non-coding RNA UCA1 promotes malignant phenotypes of renal cancer cells by modulating the miR-182-5p/DLL4 axis as a ceRNA. *Mol. Cancer* 19:18. doi: 10.1186/s12943-020-1132-x
- Wang, Y. L., Liu, J. Y., Yang, J. E., Yu, X. M., Chen, Z. L., Chen, Y. J., et al. (2019). Lnc-UCID promotes G1/S transition and hepatoma growth by preventing DHX9-mediated CDK6 down-regulation. *Hepatology* 70, 259–275. doi: 10.1002/hep.30613
- Wu, Y. M., Su, F., Kalyana-Sundaram, S., Khazanov, N., Ateeq, B., Cao, X., et al. (2013). Identification of targetable FGFR gene fusions in diverse cancers. *Cancer Discov.* 3, 636–647. doi: 10.1158/2159-8290.CD-13-0050
- Yang, J., Qiu, Q., Qian, X., Yi, J., Jiao, Y., Yu, M., et al. (2019). Long noncoding RNA LCAT1 functions as a ceRNA to regulate RAC1 function by sponging miR-4715-5p in lung cancer. *Mol. Cancer* 18:171. doi: 10.1186/s12943-019-1107-y
- Yu, Y., Yu, X., Liu, H., Song, Q., and Yang, Y. (2018). miR494 inhibits cancer-initiating cell phenotypes and reverses resistance to lapatinib by downregulating FGFR2 in HER2-positive gastric cancer. *Int. J. Mol. Med.* 42, 998–1007. doi: 10.3892/ijmm.2018.3680
- Yuan, L., Xu, Z. Y., Ruan, S. M., Mo, S., Qin, J. J., and Cheng, X. D. (2020). Long non-coding RNAs towards precision medicine in gastric cancer: early diagnosis, treatment, and drug resistance. *Mol. Cancer* 19:96. doi: 10.1186/s12943-020-01219-0
- Zhang, F., Wang, H., Yu, J., Yao, X., Yang, S., Li, W., et al. (2021). LncRNA CRNDE attenuates chemoresistance in gastric cancer via SRSF6-regulated alternative splicing of PICALM. *Mol. Cancer* 20:6. doi: 10.1186/s12943-020-01299-y
- Zhang, G., Li, S., Lu, J., Ge, Y., Wang, Q., Ma, G., et al. (2018). LncRNA MT1JP functions as a ceRNA in regulating FBXW7 through competitively binding to miR-92a-3p in gastric cancer. *Mol. Cancer* 17:87. doi: 10.1186/s12943-018-0829-6

- Zhang, M., Muralimanoharan, S., Wortman, A. C., and Mendelson, C. R. (2016). Primate-specific miR-515 family members inhibit key genes in human trophoblast differentiation and are upregulated in preeclampsia. *Proc. Natl. Acad. Sci. U.S.A.* 113, E7069–E7076. doi: 10.1073/pnas.1607849113
- Zhang, Y., Zhang, X., Cai, B., Li, Y., Jiang, Y., Fu, X., et al. (2021). The long noncoding RNA lncCIRBIL disrupts the nuclear translocation of Bclaf1 alleviating cardiac ischemia-reperfusion injury. *Nat. Commun.* 12:522. doi: 10.1038/s41467-020-20844-3
- Zhang, Z., and Wang, H. (2021). HCP5 promotes proliferation and contributes to cisplatin resistance in gastric cancer through miR-519d/HMGA1 axis. *Cancer Manag. Res.* 13, 787–794. doi: 10.2147/CMAR.S289997
- Zhao, X., Su, L., He, X., Zhao, B., and Miao, J. (2020). Long noncoding RNA CA7-4 promotes autophagy and apoptosis via sponging MIR877-3P and MIR5680 in high glucose-induced vascular endothelial cells. *Autophagy* 16, 70–85. doi: 10.1080/15548627.2019.1598750
- Zhou, C., Yi, C., Yi, Y., Qin, W., Yan, Y., Dong, X., et al. (2020). LncRNA PVT1 promotes gemcitabine resistance of pancreatic cancer via activating Wnt/beta-catenin and autophagy pathway through modulating the miR-619-5p/Pygo2 and miR-619-5p/ATG14 axes. *Mol. Cancer* 19:118. doi: 10.1186/s12943-020-01237-y
- Zhu, G., Luo, H., Feng, Y., Guryanova, O. A., Xu, J., Chen, S., et al. (2021). HOXB1LNC long non-coding RNA activation promotes leukemogenesis in NPM1-mutant acute myeloid leukemia. *Nat. Commun.* 12:1956. doi: 10.1038/s41467-021-22095-2

Conflict of Interest: The authors declare that the research was conducted in the absence of any commercial or financial relationships that could be construed as a potential conflict of interest.

Copyright © 2021 Chen, Li, Tan, Li, Zhao, Fan, Zhang, Zhao, Liu and Wang. This is an open-access article distributed under the terms of the Creative Commons Attribution License (CC BY). The use, distribution or reproduction in other forums is permitted, provided the original author(s) and the copyright owner(s) are credited and that the original publication in this journal is cited, in accordance with accepted academic practice. No use, distribution or reproduction is permitted which does not comply with these terms.